CHAPTER ONE HUNDRED FIFTY

ASPECTS OF WAVE CURRENT BOUNDARY LAYER FLOWS

Felicity C. Coffey and Peter Nielsen

ABSTRACT

   Field measurements of steady current profiles under the
influence of waves are described, including a technique for
obtaining an extra independant estimate of the friction
velocity. Field and laboratory measurements are analysed for
the effect on apparent bed roughness by superimposing waves
on a current. Finally the applicability of the eddy
viscosity concept to combined flows is examined. The
conclusion is that in general, different eddy viscosities
must be applied to different flow components.

INTRODUCTION

   The process of sediment transport and the resulting
erosion or sedimentation problems in coastal areas is most
often the result of a combined effort by waves and steady
(or quasi steady) currents. It is therefore desirable for
the coastal engineer to be able to model the flow near a
movable bed under combined flows. The aim of this paper is
to review, what is known today about wave current boundary
layer interaction, and what seems to be needed on the
experimental side.
   Waves and currents interact in two different ways.
Firstly, there is the strong and fairly obvious shoaling and
refraction effect on waves that propagate through areas with
varying current speed. This effect results from interaction
throughout the water column, and the current speed near the
surface tends to be the most important. Secondly, there is
the interaction in the bottom boundary layer, where the
waves tend to dominate and modify the current destribution.
The present paper deals entirely with the latter process.
   Since short periodic flows develop thinner boundary
layers in accordance with

$$\delta = \sqrt{\nu_T T} \qquad\qquad (1)$$

   Coastal Studies Unit, Department of Geography, University
of Sydney, N.S.W. 2006, Australia.

and thus penetrate better towards the bed, there is a general tendency for the waves to dominate this layer. In equation (1), δ is the boundary layer thickness, ν_T is the eddy viscosity, and T is the flow period.

The structure of the wave boundary layer is most often unaffected by even a fairly strong current, while the current profile always shows considerable influence from the waves under naturally occurring conditions. Figure 1 is a simplistic resume of the effects of waves on a steady current.
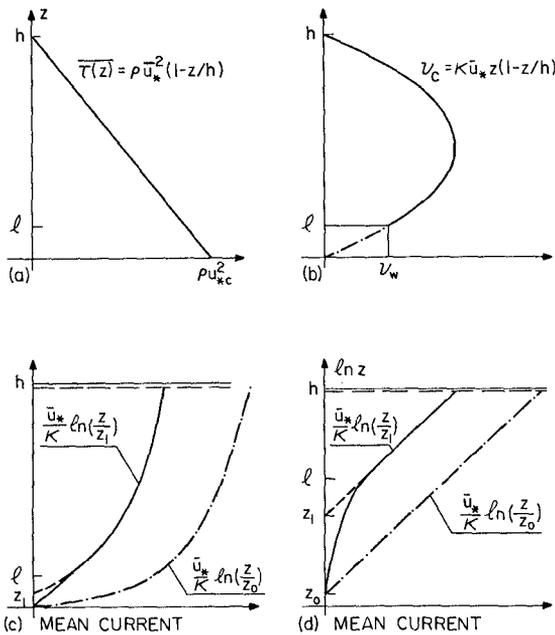

Figure 1: Influence of waves on the steady current profile. (b): The waves create extra eddy viscosity near the bed. (c) and (d): The upper part of the current profile maintains its logarithmic shape, but is shifted towards lower values, and the zero intercept is consequently increased considerably, $z_1 \gg z_0$

It is easier to get a clear idea of what is going on if the steady friction velocity $\bar{u}_*$ is thought of as a fixed

quantity. That is, we may think of flume experiments where
the slope of the mean free surface is kept constant while
different wave conditions are enforced.
   We assume that the steady shear stress is linearly
distributed (Figure 1a),

$$\tau(z) \quad = \quad \rho \, \bar{u}_*^2 \, (1-z/h) \tag{2}$$

Deviations from this may occur in the upper layers due to
gradients in wave radiation stress, but such deviations will
be small in and near the bottom boundary layer. The eddy
viscosity induced by the undisturbed steady flow is assumed
to have the form

$$\nu_T = \mathscr{K} \, \bar{u}_* \, z \, (1-z/h) \tag{3}$$

and (2) and (3) will lead to the familiar logarithmic
current profile

$$\bar{u}(z) \quad = \quad \frac{\bar{u}_*}{\mathscr{K}} \ln\frac{z}{z_0} \tag{4}$$

where $\mathscr{K}$ is von Karman's constant and z_0 is the zero
intercept (Figure 1c,d) of the logarithmic profile. The
primary effect of superimposing waves on $\bar{u}$ comes from
increasing the mixing intensity in a thin layer near the bed
(Figure 1b), which results in smaller velocity gradients for
a fixed $\bar{u}_*$.

$$\frac{\partial \bar{u}}{\partial z} = \frac{\tau/\rho}{\nu_T} \sim \frac{\bar{u}_*^2}{\nu_T} \tag{5}$$

Thus the current velocity will grow more slowly with z
through the lower layer when waves are present (Figure 1
c,d). Outside the wave boundary layer, the waves will not
contribute significantly to the eddy viscosity, and
therefore, the shape of the current profile will be
unchanged. It can be described by

$$\bar{u}(z) \quad = \quad \frac{\bar{u}_*}{\mathscr{K}} \ln\frac{z}{z_1} \tag{6}$$

Hence the only difference from the undisturbed current
profile (4) is that z_0 has been replaced by the considerably
larger z_1 .
   Such changes of the outer steady current profile have
been observed in the field by several authors e.g. Cacchione

and Drake (1982) and Grant et al (1983). Laboratory
measurements by van Doorn (1981,1982) and by Kemp and Simons
(1982,1983) also show this general trend.
   The vertical extent of the logarithmic layer is from the
top of the wave boundary layer to elevations where the waves
or other phenomena start to cause deviations from the linear
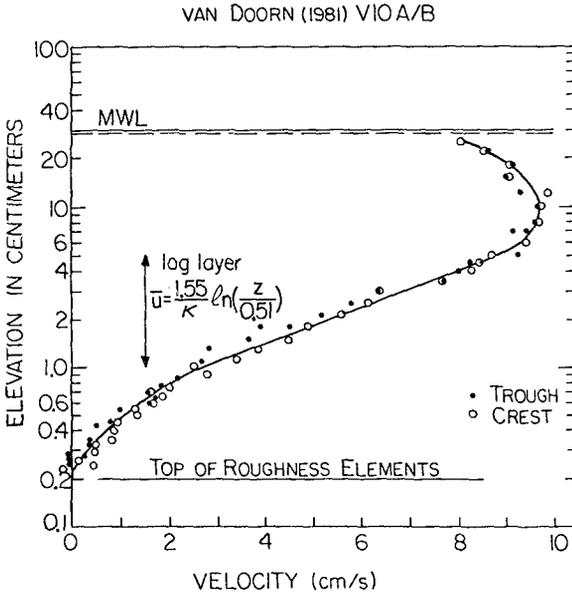shear stress distribution, as seen in figure 2.

VAN DOORN (1981) VIO A/B

Figure 2: Steady current velocities in the
presence of waves. In this case the
intercept elevation was increased from $z_0 =$
0.07cm to z_i = 0.51cm due to the presence
of waves.

   The relative change of the zero intercept (z_i/z_0) depends
mainly on the relative current strength $\bar{u}_*/A\omega$, but also on
the relative roughness r/A and the direction of the currents
relative to the waves. A is the semi excursion in the wave
motion just above the wave boundary layer and ω is the
angular velocity ($\omega=2\pi/T$), r is the hydraulic roughness of
the bed.

FIELD EXPERIMENTS

In the literature combined wave current flows are approached from two perspectives. Namely, the influence of waves on a steady flow and the influence of a current on an oscillatory flow. Field observation of oscillatory boundary layers is generally a problem as it is difficult to fit accurate current meters into the thin wave boundary layer. Thus the field experiments presented here were concerned with the measurement of steady flows under the influence of waves.

Normally, the steady flow component in the field, as well as in the laboratory, shows a nicely logarithmic behaviour over a considerable fraction of the depth, (Figure 2) which gives us the friction velocity from the slope and an apparent roughness from the z-intercept, see Figure 1.

In our experiments the steady flow component was measured by an array of five Hales and Rogers propeller flow meters. The flow meters have an inner diameter of 6cm. Simultaneous readings were obtained by storing the voltage output of each flow meter in capacitors and reading alternatively from a digital display. The flow meter output was filtered electronically over a 100s time period and the sampling interval was approximately 1 minute.

Steady flow calibration of each flow meter was performed before and after each field experiment. The flow meters were found to have a very good, linear response. Experiments were also conducted to investigate the effects of waves on the instruments' steady flow response. These effects need to be taken into account when looking at the data.

Field sites with a strong unidirectional current in association with either parallel or normal wave propagation were selected in order to obtain well controlled field experiments. The codirectional and opposing currents to direction of wave propagation were observed in the tidal channel at Port Hacking, South of Sydney, Australia. The water depth ranged between 1.1 to 2.1m and the sediment diameter was approximately 0.28mm. The average wave period and significant wave height ranged between 7 to 10s and 20 to 61cm, respectively. Well rounded ripples were generally observed and were 2-6cm high and 9-40cm long.

To observe perpendicular currents to wave direction, experiments were carried out in rip feeder channels inshore of a bar. Palm Beach, Warriewood Beach and Werri Beach, near Sydney, were selected. During some experiments currents up to 1 m/s were experienced. The water depth was approximately 1.2m and the sediment, slightly coarser than that found in the tidal channel, had an average diameter of 0.46mm. The average wave period and significant wave height ranged between 7 to 11s and 25 to 50cm, respectively. Ripple geometry varied greatly. Large well rounded ripples with height 10cm and length 90cm were observed as well as small, sharp crested, wave generated ripples with height 2cm and length 10cm.

Time averaged values of the bed shear stresses were
determined in the field by measuring the mean water surface
slope using the so-called "Barometer". The "Barometer",
Figure 3, consists of a set of vertical glass tubes which
enable us to read the difference in mean water level between
different locations. From the bottom of the tubes run
plastic hoses out to different locations. The distance
between the hose outlets is approximately 50 m. The tubes
are connected at the top so that the air pressure is the
same in all of them. We use two tubes for each location in
order to check that the instrument is working
satisfactorily. The water level should be the same in each
pair. Water level oscillations within the tubes are not
perceptible. The bed shear stresses or the friction velocity
can be determined from the surface slope, S, via

$$\tilde{u}_*^2 \;=\; -Sgh \hspace{4cm} (\,7\,)$$

60 cm

GLASS
TUBES
$\emptyset$ 25 mm
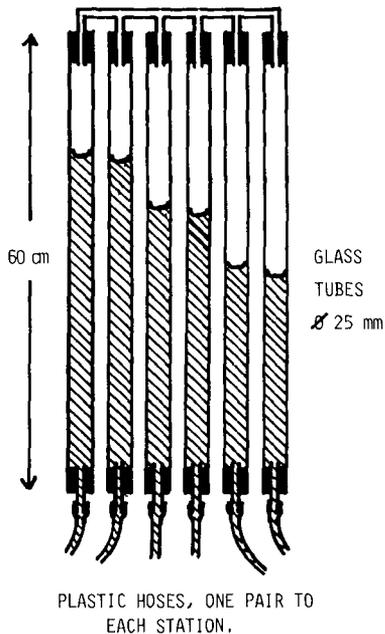
PLASTIC HOSES, ONE PAIR TO
EACH STATION.

Figure 3: The Barometer. Differences in
mean water level between the various
stations are shown by the water levels
in the vertical glass tubes.

We can compare the friction velocity derived from the
"Barometer" measurements with the friction velocity obtained
from the observed velocity distribution. This is a valuable
check. Note, however, that the "Barometer" can only be used
in situations where the surface slope is the sole driving
force of the current. In the situation where the waves
arrive obliquely to the shoreline the radiation stress
becomes a contributing driving force of the longshore
current.

EMPIRICAL KNOWLEDGE ABOUT THE APPARENT ROUGHNESS, z_1

Figure 4 shows tests 7-19 and laboratory data from the
literature plotted for apparent roughness z_1 against
relative current strength, $\bar{u}_* / A\omega$. z_1 is nondimensionalized
by the fixed bed roughness index, $8\eta^2/\lambda$, suggested by
Nielsen 1983. η is the ripple height and λ is the ripple
length. The relative current strength is the ratio between
the current friction velocity $\bar{u}_*$, and the near bed
horizontal velocity due to waves, $A\omega$. The results show that
with increasing wave dominance z_1 increases. This has been
observed by Kemp and Simons (1982,83). However, for the
current following the waves, marked by the dots, the
relationship is not clear and for perpendicular currents
(the triangles) this relationship may not hold at all. Thus
what we can see from this graph is that the relative
orientation of waves and currents is important. More
measurements are needed. The fixed bed roughness index
appears to be a satisfactory scaling parameter for four of
the perpendicular current observations, which flowed over
sharp crested ripples. These lie in the vicinity of the
laboratory data which used fixed roughness elements.
However, the majority of field observations with well
rounded ripples lie well below the laboratory data. This
indicates that for these cases the relevant scaling
parameter is the grain size rather than the ripple geometry.

WAVE BOUNDARY LAYER STRUCTURE

The wave induced velocity $u(z,t)$ inside the wave boundary
layer differs from the corresponding free stream velocity u_∞
(t) with respect to both magnitude and phase. This makes it
somewhat complicated to describe the structure of the flow.
We shall use the formalism suggested by Nielsen (in prep)
which stresses the analogy in form of all oscillatory
boundary layers with that of smooth, laminar oscillatory
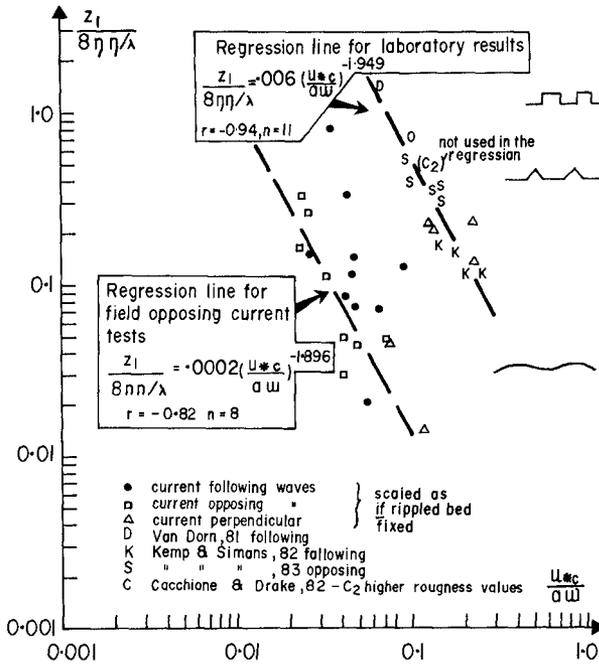flow. For simplicity, we consider only simple harmonic flow

Figure 4: Field and laboratory data plotted for apparent roughness $(30z_i)$ against relative current strength, $\bar{u}_* /A\omega$. z_i is nondimensionalized by a fixed bed roughness index, $8\eta^2/\lambda$, given by Nielsen 1983, where η is ripple height and λ is ripple length.

With increasing wave dominance z_i increases. We find two populations of data. The upper set contains laboratory data and four field measurements of perpendicular flows with sharp crested ripples. The lower group consists entirely of field measurements where well rounded ripples were observed. This suggests that when the ripples are rounded, the hydrodynamic roughness is determined by grain size rather than ripple geometry.

or the first harmonic of more complicated flows, and define the non dimensional velocity deficit $D(z)$ by

$$u(z,t) \;=\; [1-D(z)]A\omega e^{i\omega t} \tag{8}$$

D is unity at the bed and zero at infinity, so that the free stream velocity corresponds to $A\omega e^{i\omega t}$.
    For smooth, laminar flow, D is given by

$$D(z) \;=\; \exp\left[-(1+i)\frac{z}{\sqrt{2\sqrt{\nu/\omega}}}\right] \tag{9}$$

see e.g. Lamb (1945). Equation (9) shows that argument and magnitude of D are two sides of the same thing in the sense that

$$\ln D \;=\; \text{Arg } D \tag{10}$$

    Figure 5 shows the identity (10) for a rough turbulent oscillatory flow measured by van Doorn (1982).
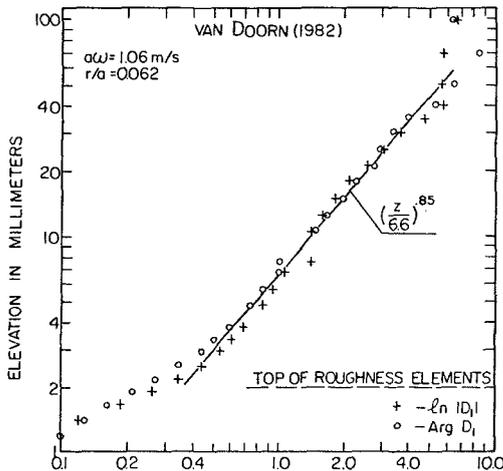

Figure 5: The identity (10) which is an analytical result for smooth laminar flow holds for most turbulent flows as well.

As pointed out by Nielsen (in prep), this identity holds
for many turbulent flows as well, with a slight
generalisation in the form of D

$$D = \exp\left[-(1+i)\left(\frac{z}{z_t}\right)^p\right]$$ (11)

where the "Stokes' length" $\sqrt{2\gamma/\omega}$ is replaced by z_t which is
approximately equal to $0.095\sqrt{rA}$. The slope parameter p
varies smoothly from unity for very rough flows (A/r < 10),
to 0.32 for smooth turbulent flow.
    The fact that very rough flows have the same slope
parameter as smooth laminar flow, namely unity, is due to
the fact that in both of these two cases there is only one
vertical length scale involved. For smooth, laminar flow it
is the "Stokes' length", and for very rough turbulent flows
it is the bed roughness length.
    The validity of (10) is not disturbed by superposition of
a steady current, and the variation of D(z) changes very
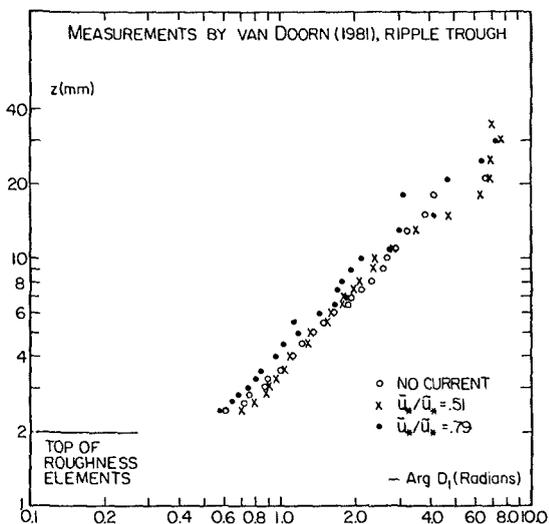little, even with a fairly strong current. See Figure 6.

Figure 6: Variation of Arg D with z for
different relative strengths of
superimposed currents. The steady
current induces very little change in
the wave boundary layer structure.

EDDY VISCOSITY IN OSCILLATORY FLOW

Shear stresses and velocity gradients in a turbulent flow are most easily related via an eddy viscosity

$$\nu_T = \frac{\tau/\rho}{\frac{\partial u}{\partial z}} \tag{12}$$

and it is therefore tempting to try and apply eddy viscosity models. It must be remembered however that ν_T is only a formal tool without strictly defined physical meaning. This becomes very clear when one considers empirical data on oscillatory flows like the ones shown in Figure 7.
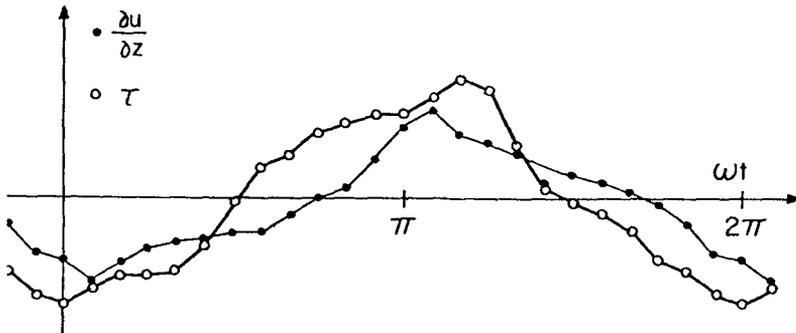

Figure 7: Time dependence of local shear stress and velocity gradient, both phase averaged. From Jonsson and Carlsen (1976) Test 1. The measurements were taken 45mm above a ripple crest.

The fact that the phase averaged values of shear stress and velocity gradients are out of phase (Figure 7) implies a somewhat radical behaviour of the eddy viscosity via the definition (12). Two interpretations are possible. One can either define the eddy viscosity as a real valued function of time, which will then have to vary approximately like $-\text{Tan}\,\omega t + \text{constant}$, see Horikawa and Watanabe (1967). The other option is to allow the eddy viscosity be a complex quantity. The latter option leads to a constant ν_T if τ and $\frac{\partial u}{\partial z}$ are simple harmonic and the angle Arg ν_T is then the phase shift between the two.

If we apply the second interpretation, measurements like the ones shown in Figure 5 correspond to complex eddy viscosities (Arg $\nu_T \neq 0$). In fact the form given by eqs. (8) and (11) corresponds to a real valued ν_T only when p=1. In that case the eddy viscosity is a real constant given by

$$\nu_T = \omega z_t^2/2 \tag{13}$$

EDDY VISCOSITIES IN COMBINED FLOWS

   Because of its simplicity the eddy viscosity model has
been applied to combined flows by several authors in the
past: Lundgren (1972), Grant and Madsen (1979) and
Christoffersen (1982). All of these authors assumed the
existence of a "common" eddy viscosity, which would apply to
all flow components.
   This assumption seems very reasonable, but it has never
been proven. Only very recently, with the publication of the
very detailed measurements by van Doorn (1981,1982) has it
become possible to test it. The test result is stunning. It
is very clearly negative, showing that steady and
oscillatory components of the same flow correspond to very
different eddy viscosities. See Figure 8.

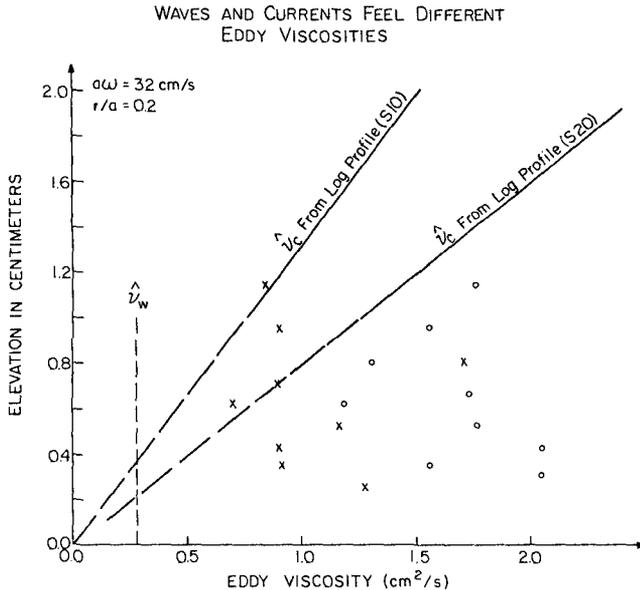WAVES AND CURRENTS FEEL DIFFERENT
EDDY VISCOSITIES

Figure 8: Eddy viscosity estimates derived from steady and
oscillatory components of the same flow. The steady
component feels 3 times larger eddy viscosities inside the
the wave boundary layer than do the waves.

   The eddy viscosity is estimated from the oscillatory
component via equation (13).
   The implication of Figure 8 is that future models of
combined flows which are based on the eddy viscosity
concept, must allow for the use of different eddy
viscosities for different flow components.

Some might then say that the use of the eddy viscosity concept is a total over simplification, and that we must turn to other models of the stress strain relation, for example, the von Karman – Prandtl mixing length model

$$\tau = \rho l^2 \left|\frac{\partial u}{\partial z}\right| \frac{\partial u}{\partial z} \tag{14}$$

However the work of van Doorn (1983) and Nielsen (in prep) show that the non linear von Karman – Prandtl model which makes analytical solution impossible, is only marginally better than the linear-eddy-viscosity-model applied by Grant and Madsen (1979). Both models predict the flow phases rather poorly. See Throwbridge (1983) or Nielsen (in prep).

CONCLUSIONS

The major effect of waves superimposed onto a current with fixed $\bar{u}_*$ is to reduce the current gradients inside the wave boundary layer. This leads to a shifting of the upper current profile towards smaller velocities. The shape of the upper current profile is unchanged because there is no wave induced mixing in this layer. One therefore finds (Lundgren, 1972) that the current profile above the wave boundary layer is logarithmic (Figure 2), and defines a friction velocity $\bar{u}_*$, by its slope and an apparent roughness ($30z_l$) by its zero intercept z_l.

The apparent roughness in combined flows is generally found to be an order of magnitude larger than the Nikuradse roughness, $30z_o$, defined by a pure current over the same bed. Field and laboratory measurements shown in Figure 4 indicate that the roughness increase z_l/z_o depends strongly on the relative current strength, $\bar{u}_*/A\omega$. The dependence may be roughly described by

$$\frac{z_l}{z_o} \sim \left(\frac{A\omega}{\bar{u}_*}\right)^{1.9} \tag{15}$$

The dependence of z_l/z_o on the relative direction of waves and currents is so far unresolved. Thus there is a strong need for well controlled experiments with waves running at an angle to the current.

Analysis of high quality laboratory measurements reveals that the eddy viscosity concept can be applied to combined flows only with extreme caution. It is found that we must in general apply different eddy viscosities to different flow components. The measurements of van Doorn (1981,1982) show that the steady flow component feels an eddy viscosity three to four times larger than the one felt by the main oscillatory component.

REFERENCES

Cacchione, D A & D E Drake (1982): Measurements of storm-
          generated bottom stresses on the continental
          shelf. J Geophys Res, Vol 87, pp 1952-1960.
Christoffersen, J B (1982): Current depth refraction of
          dissipative water waves. Series Paper 30, ISVA,
          Tech Univ Denmark.
Doorn, Th van (1981): Experimental investigation of near-
          bottom velocities in water waves without and
          with a current. Delft Hydr Lab, Rep No M1423.
Doorn, Th van (1982): Experimenteel onderzoek naar het
          snelheidsveld in de turbulente bodem grenslaag
          in een oscillerende stroming in een golftunnel.
          Delft Hydr Lab, Rep No M1562-1b.
Grant, W D & O S Madsen (1979): Combined wave and current
          interaction with a rough bottom. J Geophys Res,
          Vol 84, No C4, pp 1797-1808.
Grant, W D, A J Williams, S M Glenn, D A Cacchione & D E
          Drake (1983): High frequency bottom stress
          variability and its prediction in the CODE
          region. CODE Tech Rep No 15, Woods Hole
          Oceanographic Inst.
Horikawa K & A Watanabe (1967): A study on sand movement
          due to wave action. Coastal Engrg in Japan,
          Vol 10, pp 37-57.
Jonsson I G & N A Carlsen (1976): Experimental and
          theoretical investigations in an oscillatory
          rough turbulent boundary layer. J Hydr Res,
          Vol 14, No 1, pp 45-60.
Kemp P H & R R Simons (1982): The interaction between waves
          and a turbulent current: waves propagating with
          the current. J Fluid Mech, Vol 116, pp 227-250.
Kemp P H & R R Simons (1983): The interaction of waves and
          a turbulent current: waves propagating against
          the current. J Fluid Mech, Vol 130, pp 73-89.
Lamb H (1945): Hydrodynamics. 6th ed, Dover Pub, New York.
Lundgren H (1972): Turbulent current in the presence of
          waves. Proc 13th Int Coastal Engrg Conf,
          Vancouver, pp 623-634.
Nielsen P (1983): Analytical determination of wave height
          variation due to refraction, shoaling, and
          friction. Coastal Engrg, Vol 7, pp 233-251.
Nielsen P (in prep): On the structure of oscillatory
          boundary layers. Submitted to Coastal Engrg.
Throwbridge J H (1983): Wave-induced turbulent flow near
          a rough bed: implications of a time-varying eddy
          viscosity. PhD thesis, Woods Hole Oceanographic
          Inst, WHOI-83-40.